Performance model of SITELLE, a wide-field imaging FTS for the study of astronomical objects.

Julie Mandar[1,2], Frédéric Grandmont[2], Simon Thibault[1], Laurent Drissen[1]

[1] *Département de physique, de génie physique et d'optique, Université Laval 1045 avenue de la médecine, Québec, Canada*
[2] *ABB, 300-585 Bd Charest Est, Québec, Canada – julie.a.mandar@ca.abb.com*

Abstract: We are developing a dedicated performance model for SITELLE. We study the sensitivity in wavefront and misalignment to choose the best configuration. As SITELLE is particularly sensitive to vibrations we analyze the impact of fluctuations in OPD.
OCIS codes: (300.6300) Fourier transforms Spectroscopy; (300.6550) visible spectroscopy; (350.1260) Astronomical optics

1. SITELLE features and performance model direction

SITELLE [1] is a new imaging Fourier transform spectrometer to be installed at the end of 2012 at the Canada-France-Hawaii Telescope. This instrument will be used for the analysis of visible emission lines (360 nm to 920 nm) in a large field of view (12 arc minutes square), imaged on a 2048x2048 CCD.

Astronomers have to compete for the available observing time on a telescope. The evaluation process requires them to submit a proposal describing the quality of sky and the required time as well as the aim of the observation. Consequently, they need a time exposure and signal-to-noise ratio (SNR) calculator that is now part of each astronomical instrument. The final aim of the performance model of SITELLE is intended to be the heart of this simulator. Moreover, the development of its modules is also useful to guide the design of the instrument, as explained in this paper.

One of the special features of this instrument is the need of high efficiency at short wavelengths, as astronomers have a strong interest in the study of the [OII] weak emission line at 372.7nm (i.e. 26 830 cm^{-1}). Therefore the first step in performance modeling was to guide the choice of a configuration, between flat-mirror and retro-reflector type interferometer, to allow high transmission and modulation efficiency in the near-UV.

Another aspect to consider in the choice of the configuration is that the scene intensity may vary during the acquisition of an interferogram (typically 4 hours) because of airmass changes or sky transparency fluctuations. To get rid of those fluctuations the idea is to recover and combine the two output ports of the interferometer such that the source fluctuations can be distinguished from the true interference record. A four port flat-mirror configuration can be achieved by using the interferometer off-axis at the expense of more stringent limitations on spectral resolution. Achieving four ports with retro-reflector interferometers doubles the size of the instrument but allows to split and to recombine the light with one single substrate, keeping the high resolution power, and needs no dynamic alignment servomechanism.

Because of the high cost of a night at the telescope, astronomers always seek the most efficient way to conduct observations. Many faint targets benefit from using a band-pass filter to restrict the spectral range and allow spectral folding which significantly reduces the number of interferogram points (images) required for a given resolution. In this sub-sampling approach, contiguous frame integration is not possible (no or poor modulation recorded) and low duty-cycle is unacceptable. Therefore a step-scan mechanism is needed and its performance must be accurately modeled.

Individual steps of an acquisition can last more than one minute during which time the tracking of the astronomical object can create weak vibrations affecting stability at nanometer level. In such conditions, jitters in optical path difference (OPD) can become a critical source of noise that we need to control in order to stay photon noise limited and avoid «ghost lines».

2. Modulation efficiency performance and preference for an off-axis flat mirror configuration

Wavefront errors contribute to a difference of the OPD in the aperture. The resulting signal is given by integrating the OPD over the aperture. In our goal to compare flat-mirror and retro-reflector configurations, we attempt to compute the total wavefront error, related to various components. The followed method is described in [2].

We can see in figure 1 that the number of reflections in the interferometer plays a major role. Despite the need of a second substrate for compensation in the flat-mirror configuration, a cube-corner configuration will require reflectors at λ/40 PV to reach the performances of a flat-mirror configuration at λ/20. The roof-top case was also studied and showed median results.

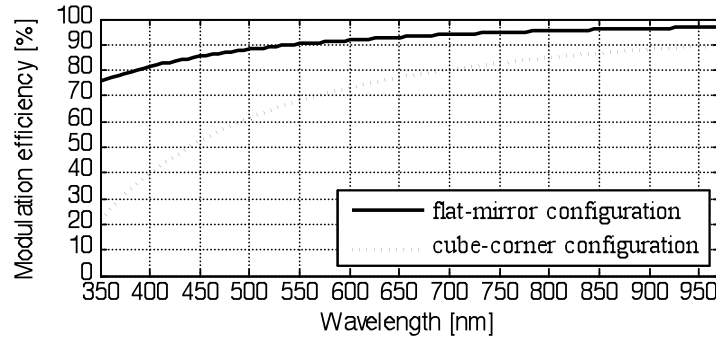Figure 1: Comparison of configurations on the modulation efficiency due to wavefront errors of λ/20 PV optical flatness, including specification of the optical component and all distortions induced by the coating deposit or the mechanical mounting.

Cube corner beam deviation and flat-mirror misalignment behave the same way. Tilt misalignment contributes to a gradient of OPD in the pupil. The resulting signal is given by integrating this OPD slope over the pupil. We studied the particular case of the ring shape aperture, as the CFHT has an obscuration ratio of 19.4 %. This expression is shown to depart slightly from the classic expression for circular aperture, available in the literature.

$$ME_{tilt} = \frac{2r_1^2 Jinc\ (2\pi\sigma_0\alpha\, r_1) - 2r_2^2 Jinc\ (2\pi\sigma_0\alpha\, r_2)}{r_1^2 - r_2^2} \qquad (2)$$

α is the optical tilt between the two recombining beams of the interferometer
D_1, diameter of the primary mirror of the telescope (3.592 m at CFHT)
D_2, diameter of the secondary mirror of the telescope (1.582m at CFHT)
$r_i = 0.5 MD_i$ radii of the pupil, associated with D_1 and D_2 and M the magnification factor of the instrument

There is also a trade on the size of the pupil. A smaller pupil will allow us to have a smaller interferometer, less sensitive to tilt, but the beam divergence will be greater for the same field of view. Consequently the imaging part of the instrument will be larger and a high image quality will be harder to achieve. For a 12 arc minute field on a 3.6 meter telescope, the pupil size that minimizes the dimensions of the beamsplitter is around 90mm, corresponding to a magnification factor about 40x. For this size of pupil, a tilt of 0.5 μrad (0.1 arc second) between the two beams of the interferometer involves a loss of modulation of about 3% at 372.7nm which is used as a target case.
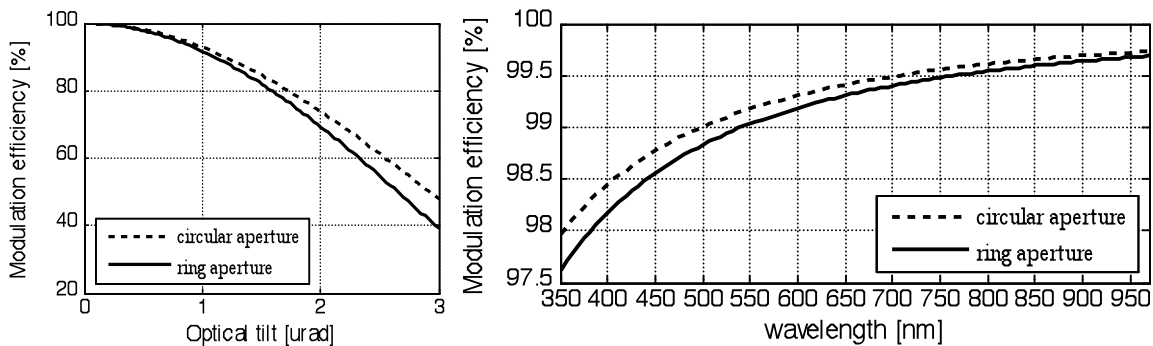

Figure 2: Modulation efficiency for a pupil of 90mm. On the left: at 372.7nm as a function of optical tilt between the two beams. On the right: for an optical tilt of 0.5 μrad as a function of wavelength.

The tilt and wavefront analyses show that the requirements in the near-UV will be achieved with cube-corners of approximately 200 mm diameter (~2.5 times the pupil size) with high quality flatness of λ/40 (all distortions included) and a beam deviation of less than 0.5μrad (0.1 arc second). Such a cube-corner would be very hard to manufacture if at all possible. Consequently our choice for a flat-mirror configuration shifts the risk from manufacture to tip-tilt servomechanism. The drawback is that the resolution will be limited by the large off-axis angle, needed to have a four ports interferometer.

3. OPD jitters study for metrology and servomechanism requirements

In this interferometer the sampling follows a step function. At each step, OPD variations will be observed over the plateau. The difference between the OPD command and the instantaneous OPD position will be time dependant and will be driven mainly by operational vibrations or external effects such as wind gust hitting the telescope. We call these positioning jitters and their first notable effect is the reduction of the modulation efficiency. In fact, the instrument integrates signal from positions around the fixed position wished for the sampling. Assuming a Gaussian distributed OPD jitters around a fixed position, the modulation efficiency loss is

$$ME_{OPDjitters} = -2\pi^2\sigma^2\sigma^2{}_{OPD}$$

where σ_{OPD} is the standard deviation of the OPD error at each step.

An 8 nm standard deviation in OPD will induce a loss of 1% on modulation efficiency at 372.7nm ([OII] emission line) which highlights the level of control stability required for SITELLE. Moreover, if the standard deviation of OPD during acquisition fluctuates between steps, the modulation efficiency will fluctuate during the whole interferogram in a choppy fashion, creating amplitude modulation. Such modulation efficiency fluctuations remain to be studied as a separate noise contributor.
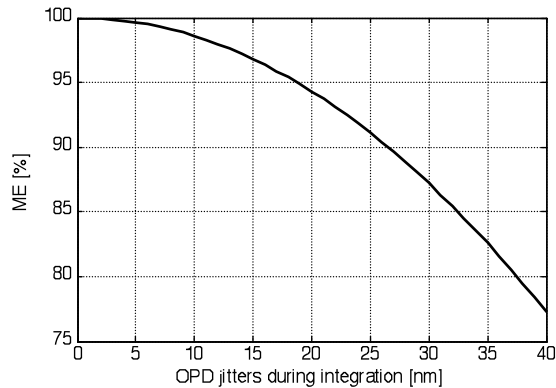

Figure 3: Modulation efficiency at 372.7nm as a function of RMS value of OPD jitters during integration at a sampling step.

It is also important to know how much the lack of precision in the sampling at regular steps will affect the measured spectra. Sampling jitter is the difference between the step command and the mean OPD realized at each step and is analog to the classic sampling error term common to speed scanning interferometers. Random errors in the sampling of the interferogram bring random frequency modulation in the measured spectrum, which lead to signal to noise ratio (SNR) reduction and may also generate « ghost lines ». The simulation shows that the SNR will decrease for higher spectral folding order (narrow filters), for smaller wavelengths, and for larger full width at half maximum (FWHM) of the instrument line shape (ILS). In fact, those conditions concur with the optimization of time spent at the telescope: small resolution power and high spectral folding order reduce the needed number of steps. Therefore, the requirement on sampling jitter can be challenging but is of the same order of magnitude, i.e. standard deviation around 10 nm sampling jitters allowed a SNR about 100.

It should be noted that this requirement is not strictly necessary for the servomechanism, but it is for the metrology of OPD. Actually, given the knowledge of the mean effective OPD at each step, the sampling jitter could be corrected by a post-processing re-sampling algorithm as is done in recent commercial instrument with Uniform Time Sampling approach.

[1] L. Drissen, A.-P. Bernier, L. Rousseau-Nepton, A. Alarie, C. Robert, G. Joncas, S. Thibault and F. Grandmont, "SITELLE: a wide-field imaging Fourier transform spectrometer for the Canada-France-Hawaii Telescope", Proc. SPIE 7735, 77350B (2010)

[2] D. R. Hearn, "Fourier Transform Interferometry," Lincoln Laboratory, MIT (1999) ADA370423